

MACHINE LEARNING ENABLED GLOBAL MAPPING OF MG-SPINEL LITHOLOGY USING CHANDRAYAAN-1 MOON MINERALOGY MAPPER (M³) DATA. M. Bhatt¹, D. Dhingra², S. Purohit³, K. Bhuva³, P. Patadiya³, H. Julasana³, U. Mall⁴. ¹Physical Research Laboratory, Ahmedabad, 380009, India. ²Department of Earth Sciences, Indian Institute of Technology Kanpur, UP 208016, India. ³Department of Computer Science, Gujarat University, Ahmedabad, India. ⁴Max Planck Institute for Solar System Research, Justus-von-Liebig-Weg3, 37077 Göttingen, Germany (megha@prl.res.in).

Introduction: A new feldspathic rock type comprising of Mg-spinel mineral was discovered on the Moon using remote sensing and subsequently reported from multiple, small localized areas [1, 2, 3, 4]. These exposures are generally associated with the thin crust regions of low-Fe terrain and expected to be globally distributed [3, 4]. The Mg-spinel detection and mapping have been carried out using the Moon Mineralogy Mapper (M³) data [5] onboard Chandrayaan-1 [6]. The presence of a strong, broad absorption band near 2 μm and the absence of any significant absorption band near 1 μm are the unique spectroscopic characteristics of Mg-spinel [7]. A systematic mapping of Mg-spinel at global scale and its association with other major lunar minerals is important for understanding its petrological significance.

We present here the first results from a machine learning enabled systematic global mapping of Mg-spinel exposures using M³ data.

Data and Method: M³ is a hyperspectral (85 bands) imaging spectrometer with a spatial resolution of 140 - 280 m/pixel in the visible-near infrared wavelength region (0.4-3 μm) [5] that flew onboard Chandrayaan-1 mission. In this work, we have utilized M³ level 2 data from optical period (OP) 1B [8].

We opted for a one dimensional convolutional neural network (CNN) which is considered to be one of the most powerful pattern recognition methods [9]. The model is trained in a fully supervised manner for improved spectral matching. For the model training, we labeled three distinct classes: (1) Mg-spinel spectral signatures extracted from already reported locations [2, 3]; (2) Pyroxene spectral signatures extracted based on the presence of absorption bands around 1 μm and 2 μm [10]; (3) Featureless reflectance spectra. We manually labeled the data into each class. The Mg-spinel spectral class consist less than 10% of spectra in comparison to other two classes. We used the Synthetic Minority Oversampling Technique (SMOTE) method to increase the number of samples in the Mg-spinel spectral class and balanced the training dataset. This approach increased the classifier robustness and accuracy. The CNN was trained with number of epochs as 5, the batch size as 100, ReLU activation function in input and hidden layers, softmax activation function for out layer, and Adam as an optimizer. For speeding up the execution, CNN approach was executed on GPU based workstation with batch-wise (13000/iteration) prediction. The model searched through 1.1 billion M³ reflectance spectra and classified a total of 2362 reflectance spectra under the

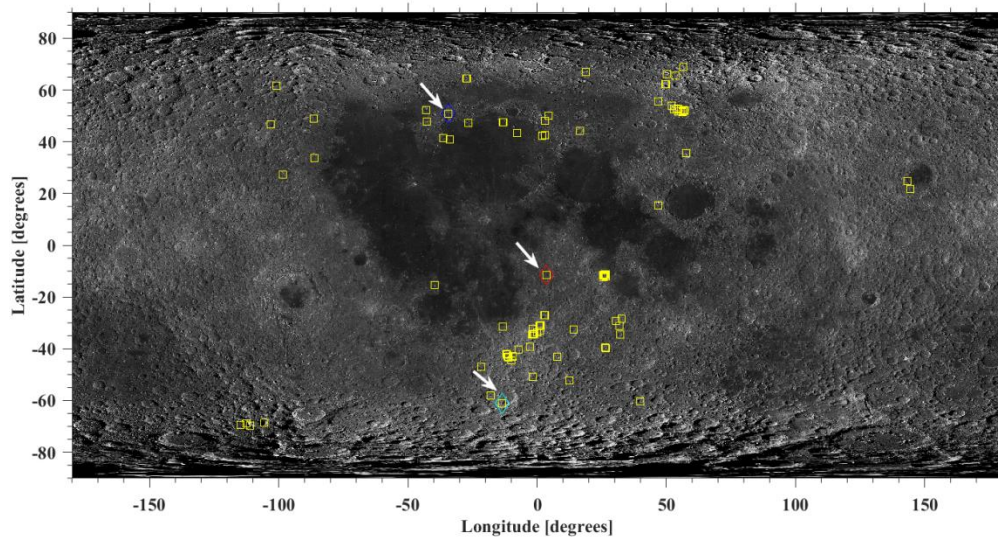


Fig. 1: Mg-spinel detections by applying a one dimensional CNN to the OP1B M³ reflectance data. The arrows are the locations from where the reflectance spectra have been extracted and shown in Fig. 2. The base map is from lunar reconnaissance orbiter wide angle camera (WAC) mosaic [12].

spectral class Mg-spinel for the spectral band parameter extraction. The data-set is further refined by examining the spectral band parameters; band center positions and the band depths. We extracted the spectral parameters using the approach adopted by [11]. Reflectance spectra with band center position $> 1.9 \mu\text{m}$ have been removed.

Results and Discussion: Fig. 1 shows select exposures of newly identified Mg-spinel locations along with already reported locations from [3]. We carried out a careful validation at the locations from [3] and found that the model successfully identified already reported exposures using OP1B M^3 data. Fig. 2 shows the reflectance spectra normalized at $1.5 \mu\text{m}$ extracted from selected locations (white arrows) in Fig. 1. The reflectance spectrum in blue in Fig. 2 is extracted from the central peak of Albategnius crater and the spectral character is comparable to [3]. The remaining two spectra (red and cyan) in Fig 2 are new identifications from high latitudes ($\pm 60^\circ$). These spectra from higher latitudes are comparatively noisy but still display the key spectral characteristics of Mg-spinel. The exposures corresponding to these spectra are located on the western wall of Rutherford crater ($61^\circ\text{S}, 12.1^\circ\text{W}$) and from an unnamed crater located at $59.9^\circ\text{N}, 34.5^\circ\text{W}$. The spatial extent in both cases is $\sim 4 M^3$ pixels.

The proposed machine learning approach identified a total of 32 new Mg-spinel locations mainly from the highlands and from mare-highland boundary regions. These results suggest that Mg-spinel exposures are even more widespread than previously thought [3, 4].

Summary and future work: This work represents our first attempt of applying machine learning techniques for identification of Mg-Spinel exposures. The model picked up all the Mg-spinel locations covered by OP1B from [3] and additionally identified several new locations typically spread over 3-4 pixels only. Such small exposures are otherwise challenging to locate manually, thereby highlighting the utility of our work in obtaining global distribution of Mg-spinel exposures. Further detailed mapping of Mg-spinel and other major lunar minerals is underway for specific sites. This work will be further extended by including the remaining M^3 reflectance data from OP2C which will include a systematic coverage of the far side. A systematic study at global scale has important implications towards understanding the origin of Mg-spinel, given that multiple hypotheses have been proposed. We will apply this developed framework to the Imaging Infrared Spectrometer [13] from Chandrayaan-2 [14] to further increase the spatial coverage.

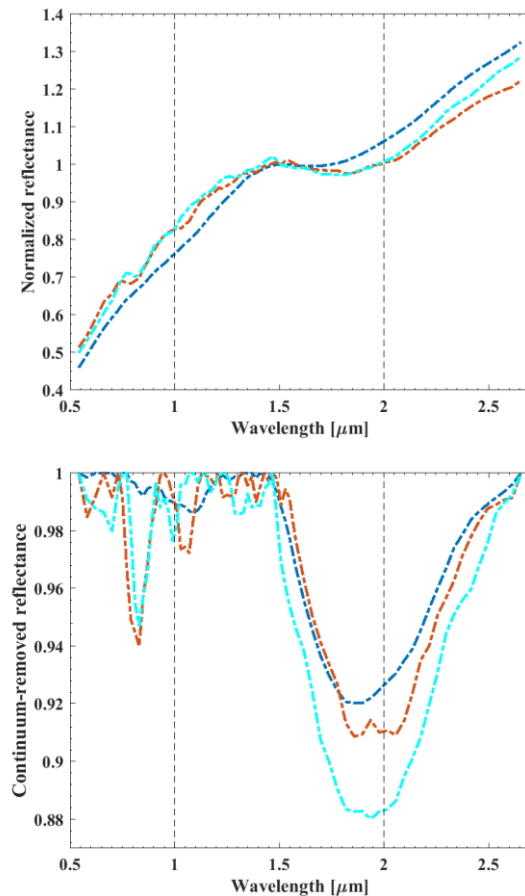


Fig. 2: Extracted reflectance spectra from locations shown in Fig. 1 (white arrows and diamonds). The top panel is normalized reflectance spectra and the bottom panel is corresponding continuum removed spectra indicating band center position less than $2 \mu\text{m}$.

Acknowledgments: Work at PRL is funded by the Dept. of Space, Govt. of India. The GPU system used belongs to the Gujarat University.

References: [1] Pieters, C. et al. (2011) JGR 116(4), 1-14. [2] Dhingra, D. et al (2011) GRL 38, L11201. [3] Pieters, C. et al. (2014) American Mineralogist, 99(10), 1893-1910. [4] Sun et al. (2017) EPSL 465, 48-58. [5] Pieters, C. et al. (2009) Current Science 96, 500-505. [6] Goswami, J. and Annadurai, M. (2009) Current Science 96, 486-491. [7] Cloutis E.A. et al. (2004) Meteoritics and Planetary Science, 39, 545-565. [8] https://pds-imaging.jpl.nasa.gov/data/m3/CH1M3_0004/. [9] J. Liu J. et al. (2017) Analyst, 2017, 142, 4067-4074. [10] Burns, R.G. et al. (1972) Proc. Lunar Science Conference, vol. 2, pp. 533-543. [11] Bhatt et al. (2018) Icarus 303, 149-165. [12] Wagner, R. V. et al. (2015) LPSC XXXXVI, 1473. [13] Chowdhury A. R. et al. (2020) Current Science, 118 (3) 368-375. [14] Vanitha, M. V. et al. (2020) LPSC 1994.